A piece-wise harmonic Langevin model of EEG dynamics: Theory and application to EEG seizure detection

Murielle Hsu, PhD

David Hsu, MD, PhD*

Department of Neurology

University of Wisconsin Hospital & Clinics

600 Highland Av, H6/526

Madison WI 53792

Ph 608-263-8551

Email hsu@neurology.wisc.edu

* Corresponding author.

Abstract

Electroencephalogram (EEG) dynamics results from the motion of charged particles in the brain. By invoking the laws of classical physics, we show that EEG dynamics obeys, at short enough times, a piece-wise harmonic Langevin equation characterized by an effective mass matrix, a piece-wise harmonic potential energy surface, a friction and random force matrix. In analyzing a sample seizure, we find with seizure onset a marked increase in frequency of encounters with inflection points on the potential energy surface, and a subtle increase in the potential energy contribution to the total force.

Keywords: EEG; seizure detection; potential energy; particle dynamics.

1 Introduction

Electroencephalogram (EEG) analysis has been applied to clinical as well as basic science studies. Clinical studies are dominated by EEG seizure detection [10] but also include studies of learning disorders [2]. Basic science studies address issues of underlying brain mechanisms such as the role of gamma band (greater than 30 Hz) oscillations in cognitive paradigms [5,7]. EEG seizure detection techniques largely depend on pattern-recognition algorithms of high sophistication [e.g., 10]. From a basic science perspective, the pattern recognition algorithms are generally not based on a physical model and do not lend themselves to physical interpretation. Newer techniques include various methods of measuring complexity as adapted from chaos theory [8,11,12,15,16], and the energy measure of Litt and coworkers [13]. The measures of complexity used in chaos theory include physically suggestive parameters such as the correlation dimension, similarity, synchrony and Lyapunov exponent. These measures all show that seizure onset is associated with a decrease in complexity. Furthermore, this decrease may occur 20 minutes or more before a clinical seizure.

The power of the chaos methods is that they are based on universal properties of dynamical systems and are independent of the details of the underlying dynamics. However, when something interesting happens and is detected by a chaos theory technique, one might hope to know a little more about the details of the underlying dynamics. One must then turn to more explicit, physically based models of EEG dynamics.

Of physically based models, the most established ones are based on an analogy between electrical circuits and neuronal circuits. Prominent workers in this field include Nunez [17], who emphasizes finding "global" solutions in his equations that represent long wavelength EEG standing waves. Another approach is that of neural networks, which is a vast field of research [1]. Neural networks can be used as simply a pattern recognition technique, or it can be used to build a realistic neuronal level model of brain dynamics. Neuronal modeling is epitomized by the work of De Schutter and

coworkers [6], which has been applied to a study of cerebellar dynamics [14].

Here we offer another physically based model, drawing on an analogy between EEG tracings and the trajectory of classical particles, with each EEG channel output describing the trajectory of a 1-dimensional particle. We show how techniques developed for the analysis of liquid and solid state particle dynamics can be applied to EEG dynamics.

2 Formal theory

EEG data are measured as the difference in electric potential between one electrode and one or more other electrodes. The electric potential at position $\vec{r}_k$ due to n charges Q_i within the brain at coordinates $\vec{r}_i(t)$ ($i = 1$ to n) is given by

$$\phi_k(t) = \sum_{i=1}^{n} \frac{Q_i}{|\vec{r}_k - \vec{r}_i(t)|}. \tag{1}$$

The charge Q_i moves around in space as given by the coordinate $\vec{r}_i(t)$ but the coordinate $\vec{r}_k$ is fixed in space. The number of charged particles n is on the order of 10^{23}. The number of spatial coordinates $\vec{r}_k$ is the same as the number of charges Q_i, i.e., $n \approx 10^{23}$. Later, we will reduce this number to a more manageable number. Our approach consists of four key steps.

The first key step is that the charged particles are constrained to obey the laws of classical physics, so that $\ddot{\vec{r}}_i(t) = -m_i^{-1}\nabla_{r_i} V$ where $\ddot{\vec{r}}_i$ is the second time derivative of $\vec{r}_i$, m_i is the mass of the i^{th} microscopic particle, ∇_{r_i} is the spatial gradient with respect to $\vec{r}_i$, and V is a potential energy function. Let $\mathbf{\Phi}$ be an n-dimensional vector whose k^{th} component is ϕ_k. Taking the second time derivative of $\mathbf{\Phi}$ and using the chain rule for derivatives on V, we have

$$\ddot{\mathbf{\Phi}}(t) = -{\mathbf{M_o}}^{-1}\nabla_\Phi V, \tag{2}$$

where ${\mathbf{M_o}}^{-1} = \mathbf{S}\mathbf{S}^T$, and

$$\vec{S}_{ki} = \frac{Q_i(\vec{r}_k - \vec{r}_i)}{\sqrt{m_i}|\vec{r}_k - \vec{r}_i|^3}. \tag{3}$$

Here $\mathbf{S}$ is an n by n block matrix whose element $\vec{S}_{ik}$ is itself a 3-dimensional row vector. In Eq (2), we neglected a term on the right-hand side of the form $\dot{\mathbf{S}}\mathbf{S}^{-1}\dot{\mathbf{\Phi}}$ which can be shown, using electroneutrality and lengthscale arguments, to be much smaller than the retained term. Equation (2) has the form of a classical equation of motion of an effective particle with coordinates ϕ_k, effective mass matrix $\mathbf{M_o}$, potential energy surface V and force $-\nabla_\phi V$.

The second key step is to expand the potential energy surface V in a Taylor series in powers of $\delta\mathbf{\Phi} = \mathbf{\Phi} - \mathbf{\Phi}_o$ [cf 4,9]. Then $V(\mathbf{\Phi}) \approx V_o - \mathbf{A_o}\,(\delta\mathbf{\Phi}) + \frac{1}{2}(\delta\mathbf{\Phi})\,\mathbf{K_o}\,(\delta\mathbf{\Phi})$ where $V_o = V(\mathbf{\Phi}_o)$, $\mathbf{A_o}$ is an n-dimensional linear expansion coefficient, and $\mathbf{K_o}$ is an n by n quadratic expansion coefficient. The time period for which this expansion is valid is denoted τ_o and is found experimentally. The expansion is repeated for consecutive short periods of time, with different values for $\mathbf{A_o}$, $\mathbf{K_o}$ and V_o in each period.

The third key step reduces the number of degrees of freedom from $n \approx 10^{23}$ to a more manageable number. Denote the experimental EEG channel outputs as $X_j(t)$, $j = 1$ to N where N is the number of channels in a given montage. The X_j's are the *explicit* degrees of freedom while the remaining ϕ_j's are the *implicit* degrees. We invoke Zwanzig's Hamiltonian formulation [19], which yields a generalized Langevin equation of motion for the explicit degrees of freedom for each short interval of time from t_o to $t_o + \tau_o$, of the form:

$$\mathbf{M}\ddot{\mathbf{X}}(t) = -\nabla_X U(\mathbf{X}) - \int_{t_o}^{t} d\tau \mathbf{\Psi}(t-\tau)\dot{\mathbf{X}}(\tau) + \mathbf{F_R}(t) \tag{4}$$

where $\mathbf{M}$ is an N by N effective mass matrix, $U(\mathbf{X})$ is a potential energy function coupling only the N explicit degrees of freedom, $\mathbf{\Psi}$ is an N by N friction memory kernel, and $\mathbf{F_R}(t)$ is an N-dimensional "random force". The influence of the implicit degrees of freedom on the explicit degrees appears through the random force and the friction term. Neither the explicit nor the implicit degrees of freedom are assumed to be at thermodynamic equilibrium. In the case that the implicit degrees of freedom are stationary, $\mathbf{\Psi}$ is then related to the autocorrelation function of the random

force through the second fluctuation-dissipation theorem, $kT\mathbf{\Psi}(t) =< \mathbf{F_R}(t)\mathbf{F_R}(0) >$ where k is Boltzmann's constant, T is the absolute temperature and $< ... >$ denotes a time average [3]. The function $\mathbf{\Psi}$ decays to zero on a timescale given by the relaxation time of the implicit degrees of freedom. If this timescale is short compared to the timescale for $\mathbf{X}$, then $\mathbf{\Psi}(t-\tau) \approx 2\mathbf{G}\delta(t-\tau)$ where $\mathbf{G}$ is the friction constant matrix. The equation of motion then reduces to the simple Langevin form, $\mathbf{M}\ddot{\mathbf{X}} = -\nabla_X U(\mathbf{X}) - \mathbf{G}\dot{\mathbf{X}} + \mathbf{F_R}$. We restrict our efforts to the simple Langevin equation because it is computationally much easier to use. Since V is piece-wise harmonic within each time interval τ_o, U is also piece-wise harmonic. The equation of motion for $\mathbf{X}$ can then be written:

$$\mathbf{M}\ddot{\mathbf{X}} = \mathbf{A} - \mathbf{K}\mathbf{X} - \mathbf{G}\dot{\mathbf{X}} + \mathbf{F_R}. \tag{5}$$

The fourth key step extracts the parameters of the equation of motion from EEG data. We first define a correlation function. Let $\delta\mathbf{X} = \mathbf{X} - \langle\mathbf{X}\rangle_c$, where $\langle ...\rangle_c$ denotes a time average over t_o to $t_o + \tau_c$. Here τ_c is a correlation interval $\tau_c > \tau_o$ over which the correlation function is calculated. The correlation interval is taken longer than the fitting interval τ_o because the statistics near the end of the correlation interval is less reliable. Define an N by N time-correlation matrix for the time interval t_o to $t_o + \tau_c$ by:

$$\mathbf{C}(t) = \langle\delta\mathbf{X}(t)\delta\mathbf{X}(0)^T\rangle_c \tag{6}$$

$$= \frac{1}{\tau_c}\int_{t_o}^{t_o+\tau_c} dt'\delta\mathbf{X}(t+t')\delta\mathbf{X}(t')^T. \tag{7}$$

Then it can be shown that

$$\mathbf{M}\ddot{\mathbf{C}}(t) = -\mathbf{K}\mathbf{C}(t) - \mathbf{G}\dot{\mathbf{C}}(t) + \mathbf{C_{RX}}(t) \tag{8}$$

where $\mathbf{C_{RX}}(t) = \langle\mathbf{F_R}(t)\delta\mathbf{X}(0)^T\rangle_c$. We assume that the random force and the explicit degrees of freedom are uncorrelated (i.e., that $\mathbf{C_{RX}}(t) = 0$). If this were not so, then the random force would not be truly random. Indeed, that $\mathbf{C_{RX}}$ should ideally be zero will be taken as our numerical

optimization goal. The parameters **A**, **M**, **K** and **G** are extracted from EEG data by making $\mathbf{C_{RX}}$ as small as possible in a least squares sense. This optimization procedure can be regarded as a way of defining the implicit variables such that they are as little correlated as possible with the explicit variables.

To proceed, for each time interval define an error measure by $E = \frac{1}{2}Tr[\langle \mathbf{C_{RX}} \mathbf{C_{RX}^T} \rangle_o]$ where $Tr[...]$ indicates a matrix trace, and $< ... >_o$ denotes a time average over the fitting interval τ_o. We use standard numerical methods for minimizing E [18], obtaining values for **M**, **K** and **G** so that E is as small as possible. The vector **A** is given by $\mathbf{A} = \mathbf{M}\langle \ddot{\mathbf{X}} \rangle_c + \mathbf{K}\langle \mathbf{X} \rangle_c + \mathbf{G}\langle \dot{\mathbf{X}} \rangle_c$. The eigenvalues of the mass matrix **M** are constrained to be positive so that every effective relative mass is positive, and the sum of the masses are normalized so that the average relative mass is one in dimensionless units. Absolute masses cannot be determined because there is a free multiplicative factor in Eq (8). Because the potential energy surface is assumed to be differentiable, the matrix **K** must be symmetric. Because of time-reversal symmetry, the matrix **G** must also be symmetric. These constraints are built into the minimization procedure. If it were not for the physical constraints on **M**, **K** and **G**, the minimization procedure could be done analytically. However, these solutions would be unphysical. Once **M**, **A**, **K** and **G** are found, one can use Eq (5) to deduce the instantaneous random force, $\mathbf{F_R}$.

3 Application to seizure detection

A 6-minute sample of a right temporal seizure was analyzed. Six minutes from the same subject one hour earlier was also obtained as a baseline. EEG data were acquired digitally at 400 Hz with a notch filter of 60 Hz. Eyeblink artifact was removed by excluding the anterior electrodes, retaining N = 12 channels (T3-T5, T5-O1, T4-T6, C3-T3, T4-C4, F3-C3, C3-P3, F4-C4, C4-P4, Fz-Cz, Cz-Pz). Onset of seizure was at 90 seconds into the seizure file and is labeled by $t = 0$. The end

of the seizure was difficult to ascertain but clinically the seizure appeared to end about 90 seconds after onset. No seizure occurred in the baseline data. Time derivatives were taken by transforming the raw data into frequency space using a Fast Fourier Transform, multiplying by $(i\omega)^n$ for the n^{th} derivative, and transforming back into the time domain. A Hamming window was also applied in frequency space to exclude frequencies below 10 Hz and above 75 Hz. The time correlation interval τ_c was taken to be 320 milliseconds but only the first $\tau_o = 100$ milliseconds were used for the least squares fit.

For each fitting window, the nearest extremum of the potential energy surface is given by $\mathbf{X_o} = \mathbf{K}^{-1}\mathbf{A}$. The numerical error in the inversion of $\mathbf{K}$ is never greater than 1 part in 10^6. Each extremum can be either a maximum (a peak on the potential energy surface) or a minimum (a potential well). An extremum displacement series is constructed by tracking $|\mathbf{X_o}|$ in time. This series show large peaks in both baseline and seizure data that are one to two orders of magnitude larger than the amplitudes of the trajectories $\mathbf{X}$. The peaks are more frequent with onset of seizure. This increase is brought out by taking the median of $|\mathbf{X_o}|$ over each preceding 5 second interval, shown in Fig 1.

The contributions of the explicit degrees of freedom to the total force is given by $\mathbf{F_{ex}} = \mathbf{A} - \mathbf{KX}$, while that of the implicit degrees of freedom is given by $\mathbf{F_{im}} = -\mathbf{G}\dot{\mathbf{X}} + \mathbf{F_R}$. The relative contribution of the explicit degrees to the total force is shown in Fig 2. Comparing the 90 seconds of the seizure to 90 seconds of baseline data taken 1 hour prior to the seizure, one sees an increase in the explicit contribution from 64% to 67%, with a two-tailed paired t-test significance of 3×10^{-9}.

There is a greater than 3-fold rise in the magnitude of the force $|\mathbf{M}\ddot{\mathbf{X}}|$ with seizure onset. The relative contribution of each term on the right hand side of Eq (5) to the total force remains nearly constant through the seizure. In particular, the relative contribution of the random force to the total force remains constant at 21% with standard deviation of 1% through the seizure. The relative

magnitude $|\mathbf{C_{RX}}|/|\ddot{\mathbf{C}}|$ is a measure of the relative error of the fit. This error is on the order of 3-4% for each fitting window with standard deviation of 1% and also does not change through the seizure period.

4 Discussion

A particle dynamics approach to EEG analysis allows separation of the EEG signal into explicit and implicit contributions. Explicit degrees of freedom are coupled through potential energy terms, while implicit degrees of freedom are represented by a friction term and the random force term. The explicit degrees of freedom are those that are directly monitored by the EEG electrodes. The implicit degrees of freedom are those that are either too far away to be directly measured (e.g, the deep nuclei) or those that are non-electrical in nature. We find that the EEG signal is dominated by the explicit interactions but that there is a subtle increase in the relative contribution of explicit degrees of freedom to the total force with seizure onset. This finding is consistent with the findings of chaos theory techniques, wherein a reduction in various measures of complexity is seen with seizure onset. Since the implicit degrees of freedom represent a macroscopic number of microscopic particles, a reduction in its contribution suggests a decrease in the effective dimensionality of the coupled implicit degrees of freedom.

In addition, there is a change in the potential energy surface, manifested by an increased rate of peaks in the extremum displacement series with seizure onset. The peaks in this series are larger than the largest displacements of the EEG data itself. Thus these peaks represent extrema that are far away from the instantaneous coordinate $\mathbf{X}$. These peaks may represent encounters with inflection points on the potential energy surface, where the curvature vanishes and the inverse of $\mathbf{K}$ becomes singular. The extrapolation to the extremum then becomes unstable and $\mathbf{X_o}$ diverges. In practice, the inverse of $\mathbf{K}$ is always well-behaved because $\mathbf{K}$ is extracted from data over a period

of 100 milliseconds, during which time $\mathbf{X}$ may sample an inflection point but is not fixed to that point. It is also possible that peaks in the extremum displacement series are artifacts of increased noise with seizure onset. However, the random force $\mathbf{F_R}$ does not increase with seizure onset, which suggests that the peaks are not due to noise artifact.

One of the most exciting findings of chaos theory analysis of seizures is that changes may occur 20 minutes or more before a seizure. If these changes can be reliably detected, the possibility of aborting a seizure before it happens arises, which would have a tremendous impact on the lives of people with epilepsy. Our method in its present form is too computationally intensive for seizure prediction in this way. To analyze 60 seconds of EEG data required nine hours on a Dell Optiplex 6X260 personal computer. The numerical least squares fit, which is performed by brute force using the Fletcher-Reeves-Polak-Ribiere algorithm [18], was the time-intensive step. Approximately 900 iterations were required for each fitting window. We have managed to increase computational speed by a factor of 100 but another 100-fold increase would be necessary for online applications.

Acknowledgements

We thank Professor Robert Fisher of Stanford University for encouragement at an early phase of this work. Professor Fisher also provided EEG data, and the necessary hardware and software to begin this work. We also thank Professor James Skinner of the University of Wisconsin for critical review and helpful ideas.

References

1. MA Arbib, The Handbook of Brain Theory and Neural Networks, 2d ed. (MIT Press, Cambridge MA 2003).

2. PT Ackerman, WB McPherson, DM Oglesby, RA Dykman, EEG power spectra of adolescent poor readers, J Learning Disabilities 31 (1998) 83-90.

3. BJ Berne, GD Harp, On the calculation of time correlation functions, Adv Chem Phys 17 (1970) 63.

4. M Buchner, BM Ladanyi, RM Stratt, The short-time dynamics of molecular liquids. Instantaneous-normal-mode theory, J Chem Phys 97 (1992) 8522-8535.

5. NE Crone, L Hao, J Hart Jr, D Boatman, RP Lesser, R Irizarry, B Gordon, Electrocorticographic gamma activity during word production in spoken and sign language, Neurology 57 (2001) 2045-53.

6. E De Schutter, Using realistic models to study synaptic integration in cerebellar Purkinje cells, Reviews in the Neurosciences 10 (1999) 233-245.

7. AS Gevins, H Leong, ME Smith, J Le, R Du, Mapping cognitive brain function with modern high-resolution electroencephalography, Trends in Neuroscience 18 (1995) 429-436.

8. LD Iasemidis, JC Sackellares, HP Zaveri, WJ Williams, Phase space topography and the Lyapunov exponent of electrocorticograms in partial seizures, Brain Topography 2 (1990) 187-201.

9. T Keyes, Instantaneous normal mode approach to liquid state dynamics, J. Phys. Chem. A 101 (1997) 2921-30.

10. YU Khan, J Gotman, Wavelet based automatic seizure detection in intracerebral electroencephalogram, Clin Neurophysiol. 114 (2003) 898-908.

11. M Le Van Quyen, J Martinerie, V Navarro, M Baulac, FJ Varela, Characterizing neurodynamic changes before seizures, J Clin Neurophys 18 (2001) 191-208.

12. K Lehnertz, RG Andrzejak, J Arnhold, T Kreuz, F Mormann, C Rieke, G Widman, CE Elger, Nonlinear EEG analysis in epilepsy, J. Clin Neurophys 18 (2001) 209-222.

13. B Litt, K Lehnertz, Seizure prediction and the preseizure period, Current Opinion in Neurology 15 (2002) 173-177.

14. R Maek, E De Schutter, Synchronization of Golgi and granule cell firing in a detailed network model of the cerebellar granule cell layer, J Neurophysiology 80 (1998) 2521-2537.

15. J Martinerie, C Adam, M Le Van Quyen, M Baulac, S Clemenceau, B Renault, F Varela, Epileptic seizures can be anticipated by non-linear analysis, Nature Med 4 (1998) 1173-6.

16. V Navarro, J Martinerie, M Le Van Quyen, S Clemenceau, C Adam, M Baulac, F Varela, Seizure anticipation in human neocortical partial epilepsy, Brain 125 (2002) 640-55.

17. P Nunez, Neocortical Dynamics and Human EEG Rhythms (Oxford University Press, New York, 1995).

18. WH Press, BP Flannery, SA Teukolsky, WT Vetterling, Numerical Recipes: The Art of Scientific Computing (Cambridge University Press, New York, 1989).

19. R Zwanzig R, Nonlinear generalized Langevin equations, J Stat Phys 9 (1973) 215-220.

Murielle Hsu received her PhD in Physics from Purdue University in 1989, with a thesis on magnetic excitations in diluted magnetic semiconductors and their superlattices. She has been until 2001 a Reader in Mathematics at City University in London, studying the electronic and transport properties of metallic magnetic multilayers. She developed an interest in EEG dynamics in 2000 and is a founding member of the Neuroscience Physical Theory Group at the University of Wisconsin.

David Hsu received his PhD in Chemical Physics from Columbia University in 1986, with a thesis on the pure dephasing of optical excitations in crystals. He developed various techniques for quantum dynamical simulations before obtaining his MD at the University of Pittsburgh in 1997. He trained in Pediatrics at the University of Iowa, then in Pediatric Neurology at Stanford University, and joined the Neurology faculty at the University of Wisconsin in 2003. He is a co-founder of the Neuroscience Physical Theory Group at the University of Wisconsin.

Figure captions

1. The median of the magnitude of the extremum displacement series $|\mathbf{X}_o|$, taken over each preceding five second interval. Units are in microvolts. Solid line is the seizure data. Dotted line is baseline data taken one hour prior to onset of seizure. Onset of seizure is at $t = 0$. Seizure ends at approximately $t = 90$ seconds.

2. The relative contribution of the explicit degrees of freedom to the total force. Solid line is the seizure data. Dotted line is baseline data taken one hour prior to onset of seizure. Onset of seizure is at $t = 0$. Seizure ends at approximately $t = 90$ seconds.

Fig 1

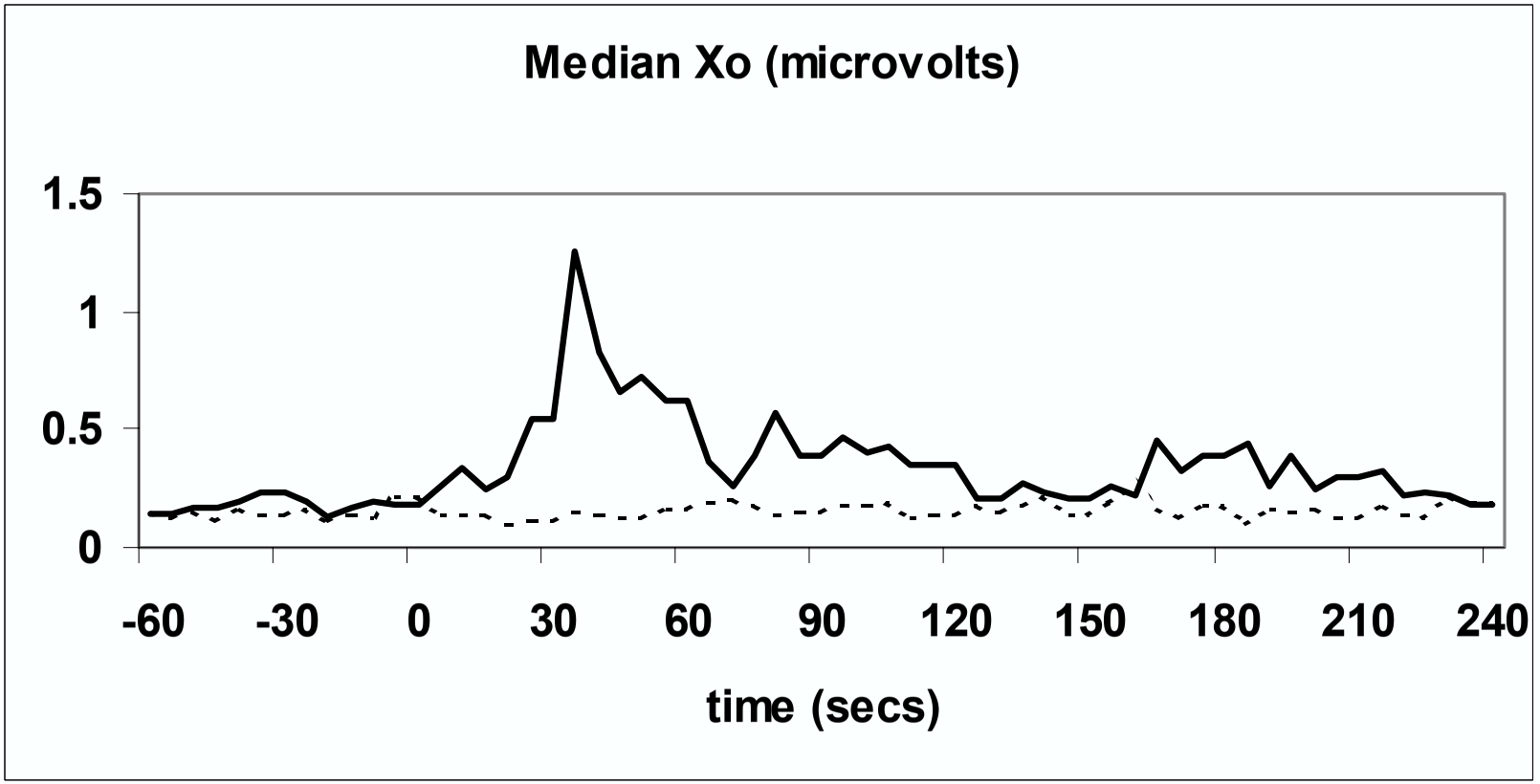
Median Xo (microvolts)
1.5
1
0.5
0
-60
-30
0
30
60
90
120
150
180
210
240
time (secs)

Fig 2

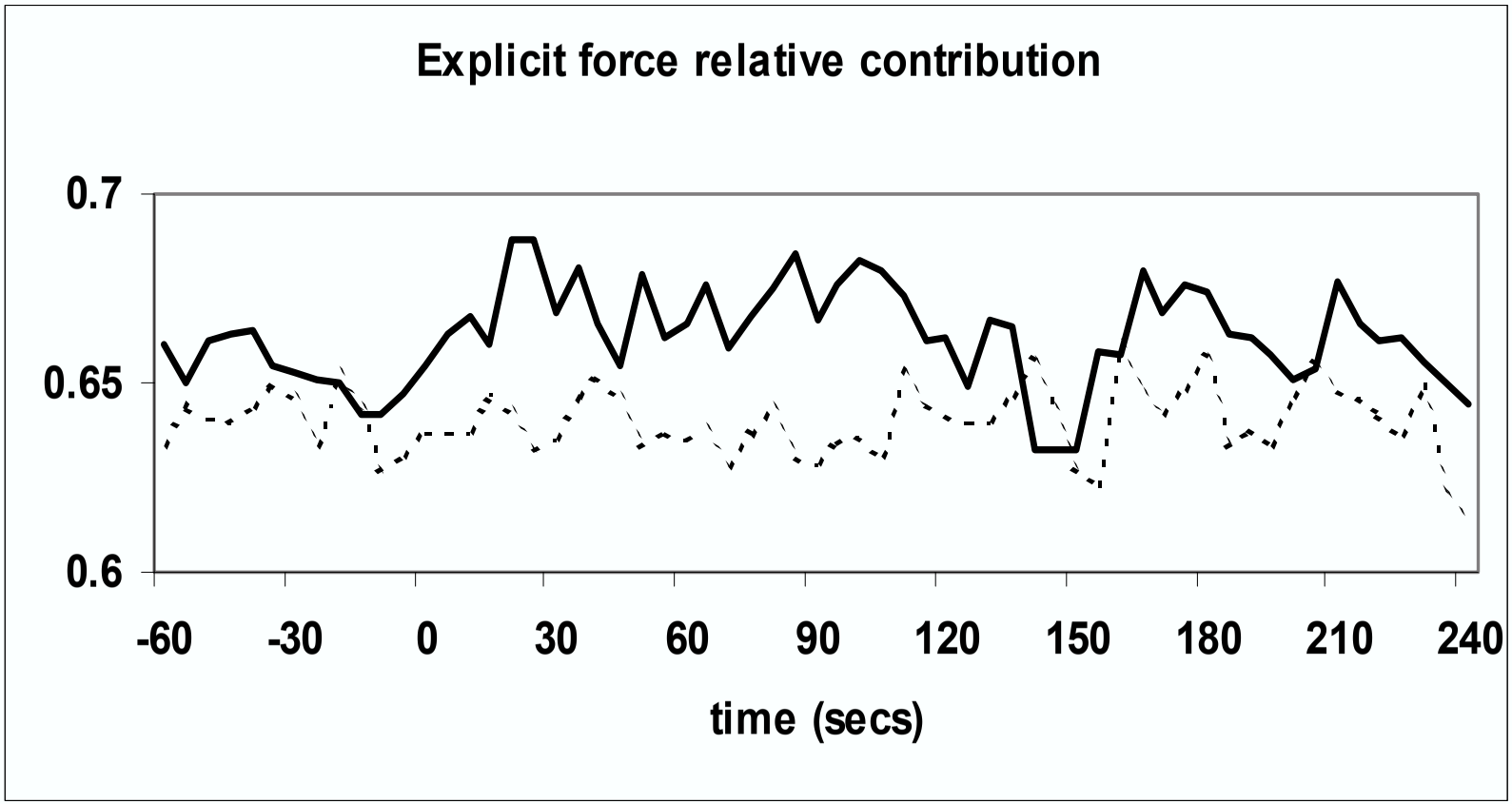
Explicit force relative contribution
0.7
0.65
0.6
-60
-30
0
30
60
90
120
150
180
210
240
time (secs)